Biochemical and Biophysical Research Communications 373 (2008) 8–13

Contents lists available at ScienceDirect

Biochemical and Biophysical Research Communications

journal homepage: www.elsevier.com/locate/ybbrc

Active site of mycobacterial dUTPase: Structural characteristics and a built-in sensor

Balázs Varga, Orsolya Barabás, Enikő Takács, Nikolett Nagy, Péter Nagy, Beáta G. Vértessy *

Laboratory of Genome Metabolism and Repair, Institute of Enzymology, Hungarian Academy of Sciences, Karolina ut 29, H-1113 Budapest, Hungary

ARTICLE INFO

Article history:
Received 13 May 2008
Available online 2 June 2008

Keywords:
Tuberculosis
Mycobacterium tuberculosis
dUTPase
Tryptophan sensor
Pyrophosphate assay
Inhibitor screening
Fluorescence spectroscopy
Enzyme kinetics
Uracil

ABSTRACT

dUTPases are essential to eliminate dUTP for DNA integrity and provide dUMP for thymidylate biosynthesis. *Mycobacterium tuberculosis* apparently lacks any other thymidylate biosynthesis pathway, therefore dUTPase is a promising antituberculotic drug target. Crystal structure of the mycobacterial enzyme in complex with the isosteric substrate analog, α,β-imido-dUTP and Mg^{2+} at 1.5 Å resolution was determined that visualizes the full-length C-terminus, previously not localized. Interactions of a conserved motif important in catalysis, the *Mycobacterium*-specific five-residue-loop insert and C-terminal tetrapeptide could now be described in detail. Stacking of C-terminal histidine upon the uracil moiety prompted replacement with tryptophan. The resulting sensitive fluorescent sensor enables fast screening for binding of potential inhibitors to the active site. K_d for α,β-imido-dUTP binding to mycobacterial dUTPase is determined to be 10-fold less than for human dUTPase, which is to be considered in drug optimization. A robust continuous activity assay for kinetic screening is proposed.

Tuberculosis is a widespread and deadly infectious disease with one third of the human population already infected [1]. Soon after the introduction of the first anti-TB drug, streptomycin, in 1943, drug-resistant strains have appeared. The subsequent introduction of isoniazid and later rifampicin seemed to have solved the problem. Uncontrolled treatment, however, has led to the rise of multi-drug-resistant TB incidence (MDR-TB: resistance to isoniazid and rifampicin and possibly other drugs). Poor compliance to the therapy using these drugs combined with the second-line antituberculotics (e.g. pyrazinamide and ethambutol) resulted in extremely drug-resistant strains (XDR-TB: resistant to at least three of the available antituberculotics including rifampicin and isoniazid) [2]. The emergence of such strains urges the development of novel drugs [3].

Thymidylate metabolism targeting is a widely used chemotherapeutic strategy both in anticancer and antimicrobial treatments [4, 5]. The usual approach is focused on thymidylate synthase, but dUTPase has also been proposed as a useful target [6, 7]. Not only does dUTPase play an important role in preventive DNA repair [8], but its targeting may also lead to a more specific inhibition blocking the thymidine biosynthesis pathway. The importance of dUTPase in *Mycobacterium tuberculosis* is highlighted by its key role in thymidylate biosynthesis. Neither dCMP deaminase nor dT kinase have been identified in the *M. tub.* genome (TubercuList World-Wide Web Server, http://genolist.pasteur.fr/TubercuList), so there seems to be no alternative pathway for dUMP formation, but through the dCTP → dUTP (catalysed by dCTP deaminase) and the subsequent dUTP → dUMP (catalysed by dUTPase) reaction pathway (Fig. 1). Thus, dUTPase provides the sole source of dTMP for DNA biosynthesis. This enzymatic activity is also found in the bifunctional dCTP deaminase/dUTPase [9].

dUTPases are mostly homotrimer enzymes with well-conserved fold [10–13]. The three active sites are constructed in a unique fashion from conserved residues, within the five hallmark dUTPase motifs (motifs 1 through 5) [14], from all the three monomers contributing to each active site. Structure-based inhibitor design against the malaria parasite *Plasmodium falciparum* dUTPase resulted in some lead molecules [7]. For such inhibitor design, species-specific characteristics are of much significance, which may allow less cross-reactivity with host (human) dUTPase.

The first report on *M. tub.* dUTPase crystal structure mapped interactions of the active site, which are largely similar in other dUTPases [12, 13, 15]. However, due to flexibility of the C-terminal region, a phenomenon usually observed in dUTPase structures, the last 10 residues could not be localized. This peptide segment is part of motif 5 and interestingly contains a His residue at the site of an otherwise strictly conserved Phe. The Phe residue has been shown to stack over the uracil ring of the substrate in both viral and

* Corresponding author. Fax: +36 1 4665465.
E-mail address: vertessy@enzim.hu (B.G. Vértessy).

0006-291X/$ - see front matter © 2008 Elsevier Inc. All rights reserved.
doi:10.1016/j.bbrc.2008.05.130

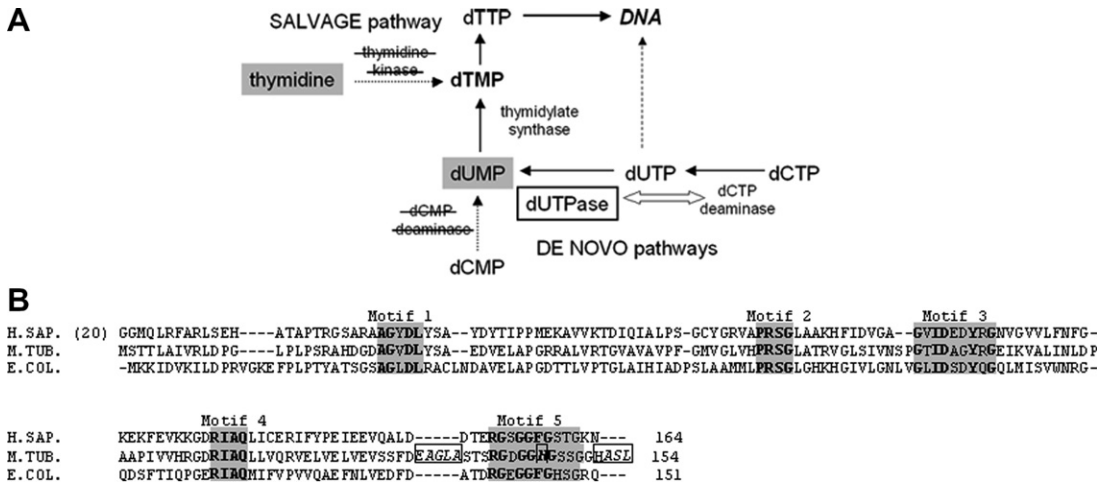

Fig. 1. (A) Pathway(s) to generate dTMP, the obligate precursor for dTTP. *M. tub.* employs only the one pathway that necessarily involves dUTPase. Genes encoding enzymes dCMP deaminase and thymidine kinase could not be identified in the *M. tub.* genome, these pathways are crossed out. Dashed line from dUTP to DNA indicates that DNA polymerase is fully capable of incorporating either thymine or uracil into DNA, to base-pair with adenine, based on relative availabilities of dTTP and dUTP. The connection between dUTPase and dCTP deaminase refers to the recently identified bifunctional enzyme in *M. tub.* [9]. (B) Alignment of human, *M. tub.* and *E. coli* dUTPases. Conserved motifs are in gray background, strictly conserved residues in bold and the species-specific loops Glu132-Ala136, and His151-Leu154 and His145 are boxed.

human dUTPase [11, 12]. The polar replacement of this residue may challenge this role. Other *M. tub.*-specific segments around the active site include a five-residue-loop and the C-terminal tetrapeptide (Fig. 1B).

We solved the crystal structure of *M. tub.* dUTPase:α,β-imido-dUTP:Mg^{2+} complex at 1.5 Å resolution, and localized the full-length C-terminal arm with the species-specific loop regions. Interactions of the corresponding residues with the other parts of the molecule are detailed, and the His145 residue, replacing the highly conserved Phe, was also localized. His145 still stacks over the uracil ring, but utilizes H-bonding for substrate accommodation, as well. A sensitive fluorescent sensor was introduced into the protein molecule by mutating this His residue to Trp allowing for the detection of binding of ligands to the active site (cf [12, 16]). The pyrophosphate assay [17] was optimized to allow continuous detection. Thus, a coupled enzymatic activity assay providing a fast, sensitive and reliable continuous detection potent for even large-scale screening is presented.

Materials and methods

Materials. Chemicals of analytical grade purity, including dUTP and the auxiliary enzymes were from Sigma–Aldrich. Phenolred was from Merck. α,β-imido-dUTP and 2-amino-6-mercapto-7-methylpurine ribonucleoside were from Jena Bioscience. Restriction enzymes and other molecular biology materials were from New England Biolabs.

Cloning and purification. Recombinant *M. tub.* dUTPase with an N-terminal 6xHis-tag was cloned, expressed, and purified as described in [18]. *Escherichia coli* strain BL21(DE3) (pLysS) was used for protein expression. The final supernatant after cell extraction was loaded on a NiNTA column (Novagen) and purified according to the Novagen protocol. Salt-wash was followed by step-wash in 50 mM Tris–HCl, pH 7.5, buffer containing 30 mM NaCl, and 50 mM imidasole. dUTPase was eluted in 0.5 M imidasole, pH 7.5, and was subsequently dialyzed into the proper buffer. To construct the His145Trp mutant, forward and reverse primers: 5′-CG GCGACGGTGGCTGGGGTTCCTCCGGCGG-3′ and 5′-CCGCCGGAGGA ACCCCAGCCACCGTCGCCG-3′, respectively, were used. Mutation was verified by DNA sequencing on both strands. The mutant was expressed and purified as the wild-type enzyme.

Protein concentration in monomers was determined by UV spectrometry using A_{280} = 2980 M^{-1} cm^{-1} and 8480 M^{-1} cm^{-1} for wild-type and His145Trp mutant, respectively, as calculated from the amino acid sequence.

Crystallization and crystallography. About 223 μM dUTPase, 1.25 mM α,β-imido-dUTP and 10 mM $MgCl_2$ in 10 mM Tris–HCl, pH 7.0, 50 mM NaCl, and 0.1 mM TCEP buffer was mixed with different reservoir solutions (cf. Supplementary Table 1). Well diffracting crystals were obtained from numerous conditions and the best crystal was selected for further analysis. Data were collected on a Rigaku R-Axis IIC imaging plate detector on a Rigaku X-ray generator. Data were evaluated using the XDS program. Structure of the dUTPase:α, β-imido-dUTP:Mg^{2+} complex was solved by molecular replacement (MOLREP), [19] using the first deposited *Mycobacterium tuberculosis* dUTPase structure (PDB ID: 1MQ7) (cf. Supplementary Table II). Data procession was done using the CCP4 program package and the Refmac software. Coordinates and structure factor data have been deposited in the Protein Data Bank with Accession Code 2PY4. Figures were produced using Pymol.

Fluorimetry. Emission spectra were recorded on a Jobin Yvon Spex Fluoromax-3 spectrofluorimeter using 10 mm path length 20 °C thermostatted cuvettes as described in [12], with the exception that during titration, emission intensity at 354 nm (slit: 5 nm) was followed. Titration data were fit to the equation describing 1:1 stoichiometry for the dissociation equilibrium with no cooperativity (as shown in Fig. 3B):

$y = s + A[(c + K + x) - ((c + K + x)^2 - 4cx)^{1/2}]/(2c)$, where x, nucleotide concentration; y, fluorescent intensity; s, intercept on y axis; A, amplitude; c, enzyme concentration; K, K_d.

Continuous dUTPase enzyme activity assays. A JASCO-V550 spectrophotometer and 10 mm path length 25 °C thermostatted cuvettes were used. The k_{cat} values in both assays were calculated using the equation: $k_{cat} = v_{init}^{*}[dUTP]/(\Delta A_{total}^{*}[dUTPase])$. Initial velocity was determined from the first 10% of the progress curve (cf. [20]).

(i) Phenolred assay was carried out according to [20] using dUTPase concentrations of 100–180 nM; dUTP at 40 μM in 1 mM Hepes, pH 7.5, buffer containing 150 mM KCl, 40 μM phenol red, and 1 mM $MgCl_2$.

(ii) Pyrophosphate assay: The EnzCheck Pyrophosphate Assay Kit (based on [17]), is only for end-point titration. In order to follow the reaction continuously, with dUTPase catalysis being the rate-

limiting step, we fine-tuned the concentrations to be: [dUTPase] = 100–180 nM, [inorganic pyrophosphatase] = 5 U/mL,[purine nucleoside phosphorylase] = 5 U/mL, [2-amino-6-mercapto-7-methylpurine ribonucleoside] = 100 μM, [dUTP] = 5 μM in 50 mM Tris–HCl, pH 7.5, 1 mM $MgCl_2$ buffer using a JASCO-V550 spectrophotometer, and 10 mm path length 25 °C thermostatted cuvettes. 2-amino-6-mercapto-7-methylpurine ribonucleoside, purine nucleoside phosphorylase, inorganic pyrophosphatase, and dUTP were added to the buffer, mixed, and allowed to equilibrate at 25 °C for a few minutes. Then measurement was started, and the reaction was initiated by quickly adding dUTPase to the cuvette (detection interrupted, as shown in Fig. 3D).

Results

Localization of the C-terminal residues in the M. tub. dUTPase:α,β-imido-dUTP:Mg^{2+} complex

The previously reported crystal structure of *M. tub.* dUTPase in complex with the substrate analog α,β-imido-dUTP and Mg^{2+} char-

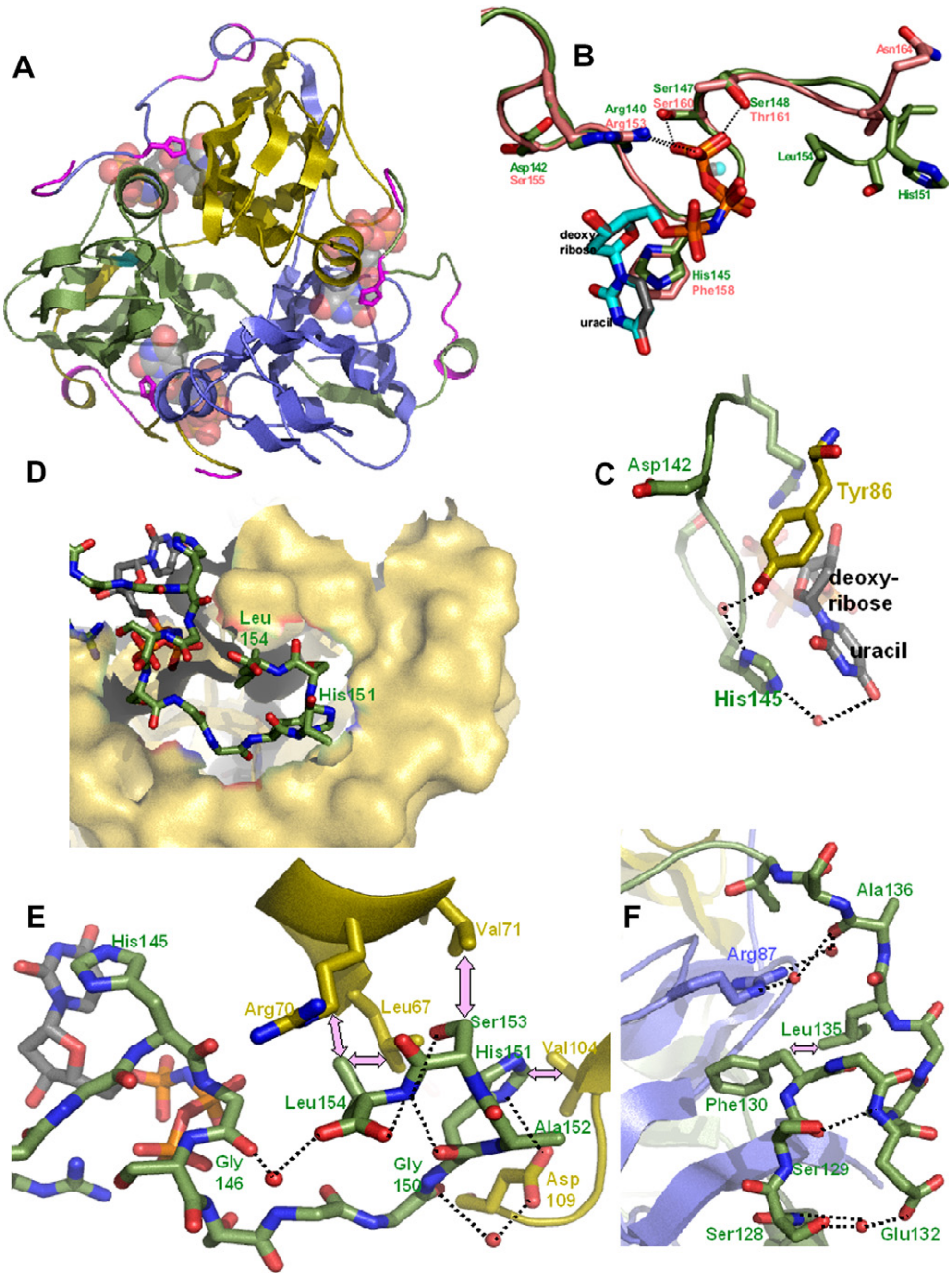

Fig. 2. Localization of the species-specific segments around the active site of *M. tub.* dUTPase. (A) Main chain fold. The three α,β-imido-dUTP molecules (transparent space-filling models with atom coded coloring (N, blue; O, red; P, orange; C, green)) are accommodated within the color-coded subunit ribbon model. Peptide backbone of the species-specific segments Glu132–Ala136, His151-Leu154 as well as the *M. tub.*-specific His145 are in magenta. B. Motif 5 residues show similar interactions with the nucleotide in both *M. tub.* and *H. sap.* dUTPases. The two structures (PDB ID 2HQU [12] and 2PY4), were superimposed. Color code: atomic coloring with green carbon for *M. tub.* protein, pink carbon for *H. sap.* protein, gray carbon and Mg(II) for *M. tub.* nucleotide, blue carbon and Mg(II) for *H. sap.* nucleotide. The His145 and Phe158 residues display equivalent stacking. (C) Close-up of uracil-stacking. (D and E) Space-complementarity (D) and interactions (E) for the back-folded *M. tub.* C-terminal tetrapeptide His151-Leu154 with the protein surface of the neighboring subunit. Dotted lines represent H-bonds and pink double arrows represent van der Waals interactions. (F) Interactions of the *M. tub.*-specific loop Glu132-Ala136.

acterized most substrate binding features and also proposed a mechanism for nucleophilic attack by an activated water molecule [13]. The mechanistic suggestion was in agreement with in-depth structural and kinetic studies performed with wild-type and active-site-mutant *E. coli* dUTPase complexes [15]. The C-terminal motif 5, one of the hallmark motifs of dUTPases, reported to be essential for catalytic activity [21, 22] could be localized only partially in this study [13]. Interestingly, within this motif 5, the usually strictly conserved Phe, coordinating to the uracil ring via stacking interactions in human and FIV dUTPases [12, 23, 24] is replaced by histidine. The effect of this polar replacement on the stacking interaction could be best studied within a high-resolution 3D structure that visualizes this segment.

To determine such a structure, we screened a wide range of crystallization buffers/precipitants (cf. Supplementary Table 1). Out of the crystals tested, the best resolution structure provided clear electron density map for the full-length C-terminal region. In this structure, the overall fold together with side chain and ligand conformations are much similar to the previously determined structure [13] (rms 0.39 angström for 1136 atoms superimposed). Fig. 2 presents the structure with close-ups for the *M. tub.*-specific loops and the C-terminal motif 5. The previously unresolved segments reveal that the His residue replacing the conserved Phe in motif 5 is situated next to the uracil ring of the substrate analog in a manner much similar to the previously observed Phe-uracil stacking in human, Mason-Pfizer monkey retroviral and feline immunodeficiency viral dUTPases (Fig. 2B) [11, 12, 24]. In addition to van der Waals stacking, polar character of this His residue also contributes to nucleotide accommodation. Imidazole nitrogen atoms engage in water-mediated H-bonding towards the O_4 atom of the uracil ring and the hydroxyl of the Tyr residue that coordinates the deoxyribose ring (Fig. 2C). Other interactions between the C-terminal motif 5 residues and the nucleotide ligand are equivalent to those found in the human enzyme [12, 16] (Fig. 2B).

The C-terminal *M. tub.*-specific tetrapeptide segment folds back and occupies a much complementary surface cavity of the neighboring subunit (Fig. 2D). Numerous interactions are realized to stabilize this back-folded conformation and to facilitate adherence of the C-terminus to the trimer surface (Fig. 2E). Main chain H-bonds connect the Leu154, His151, and Gly146 amino acids. The Ala152 main chain imino nitrogen is in water-mediated contact to Asp109 side chain of the neighboring subunit that is connected also to the His151 imidazole ring. Hydrophobic contacts are also observed between the Leu154 side chain and the methylene groups of the Arg70/Leu67 side from the neighboring subunit, while the Ser153 β-methylene is close to the Val71 γ-methylene (Fig. 2E). These multiple interactions between the C-terminal arm and the protein surface may well facilitate ordering of motif 5 upon the active site. The *M. tub.*-specific five-residue-loop (Glu132-Gly137) locally alters the peptide chain folding but residues within this segment do not show direct interactions with the active site (Fig. 2F), nor with the protein surface.

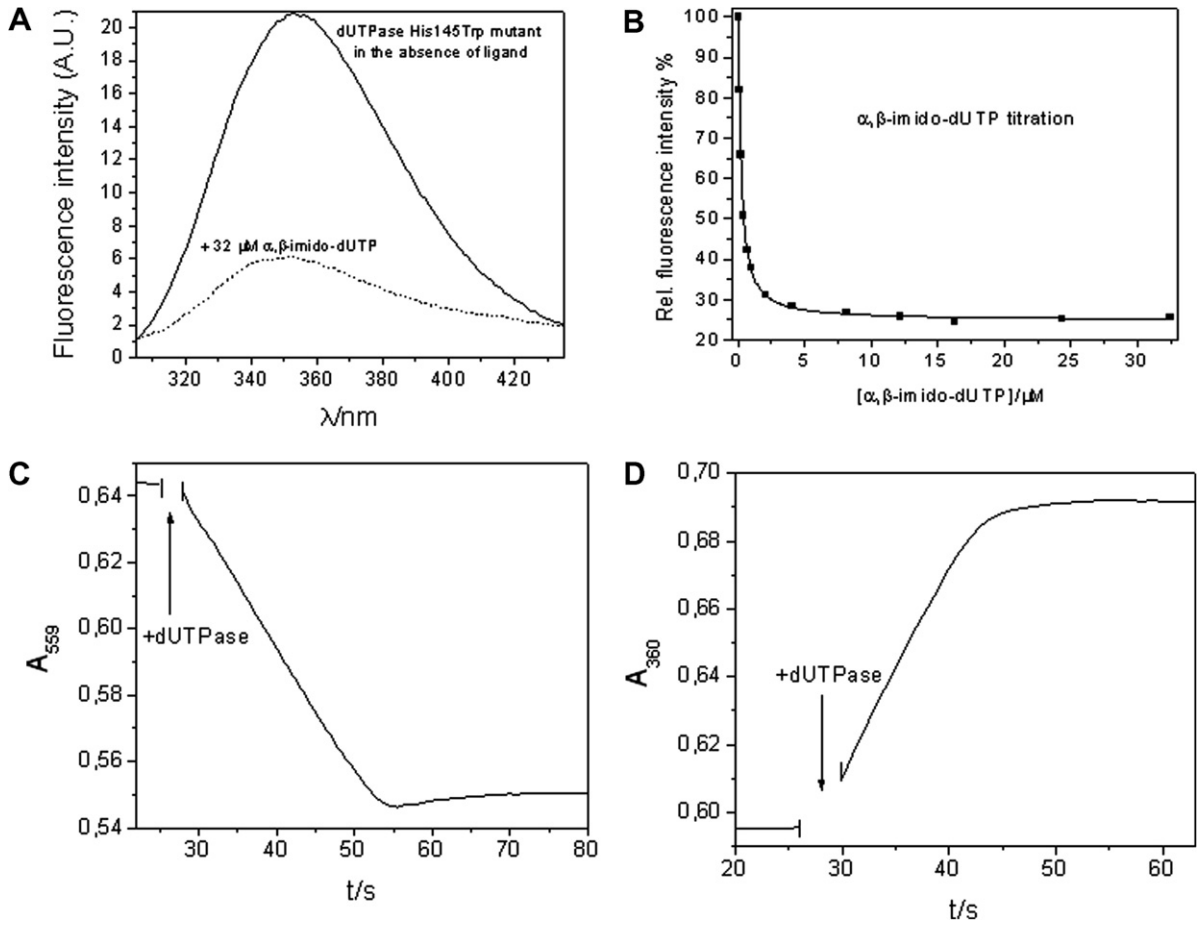

Fig. 3. (A and B) Trp fluorescence as a sensor. (A) Fluorescent spectra of *M. tub.* His145Trp mutant dUTPase apoenzyme and enzyme:α,β-imido-dUTP (saturated) complex. (B) Titration curve (data were fitted to the equation for 1:1 binding). (C and D) Comparison of the continuous phenolred (C) and pyrophosphate (D) dUTPase activity assays. Progress curves follow absorbance decrease of phenolred at 559 nm upon protonation (C); or absorbance increase at 360 nm upon methyl-thio-guanidine formation (D). About 100 nM dUTPase and either 40 μM (C) or 5 μM (D) dUTP were used.

The design of a Trp sensor

In search for active site-binder inhibitors and especially for high-throughput-screening, a simple and reliable spectral reporter within the active site is of great advantage. The uracil-stacking Phe residue in human dUTPase proved to be such a reliable sensor [12,16]. Since His145 in *M. tub.* dUTPase also stacks over the uracil, we constructed the His145Trp mutant. This replacement introduced a sensitive fluorescent label into the binding site. The steady-state kinetics showed no difference in the case of the mutant and wild-type enzyme, k_{cat} was found to be 3.7–5.8 s^{-1} for both enzymes. Substrate saturation curves showed that K_m is below 1 μM for both the wild-type and the His145Trp mutant (data not shown). Binding of the substrate analog or the product induces an intensity loss in the fluorescent signal (Fig. 3), similarly to what was found for human dUTPase [12]. The dissociation constant of the *M. tub.* dUTPase:α,β-imido-dUTP complex was determined by fluorescence titration to be 0.2 μM (also an upper limit for dUTP K_d, cf. [16]). This value is much lower than K_d of the human dUTPase:α,β-imido-dUTP complex (1.6 μM, [12]). Based on the crystal structure data, we propose that the *M. tub.*-specific His residue with its additional H-bonding and the more widespread interaction pattern between the C-terminus and the protein surface around the active site are at least partially responsible for this strengthened binding.

A robust and continuous dUTPase enzyme activity assay

For determination of enzyme kinetic parameters, the conventional phenolred indicator has so far been routinely used to follow the dUTPase reaction [25]. This indicator assay detects the proton release during the reaction as described in [20,25]. However, this assay requires about 40 μM dUTP for 0.1 total absorbance change, a concentration much oversaturating for *M. tub.* dUTPase that binds its substrate very strongly (K_d around 0.2 μM, as determined by fluorimetry). Sensitivity limit of standard spectrophotometers does not allow reliable reaction traces with [dUTP] < 4 μM. In addition, this assay is easily perturbed by minor changes in the pH upon addition of additional substances (e.g. inhibitor candidates), or by atmospheric CO_2 absorption. The disturbing effects are clearly visible at the end of the progress curve: instead of a dead-end, a negative maximum is observed (Fig. 3C). In order to increase sensitivity, reliability, and to avoid the necessity of using inert atmosphere, pyrophosphate release (product formation) was followed with coupled enzymatic reactions (cf [17]) (Fig. 3D). The optimized PP_i assay was found to be much more sensitive than the phenolred assay: 0.1 ΔA_{total} was observed by the hydrolysis of 5 μM dUTP to be compared with 40 μM in the indicator assay. The k_{cat} determined from both activity assays are the same within error, indicating that the steady-state rate of H^+ and PP_i release is the same as expected.

Discussion

The replacement of His145 by Trp proved to be a very efficient and highly sensitive label to follow ligand binding into the active site. The much strengthened binding of α,β-imido-dUTP, accounted for by the increased molecular interactions as revealed in the crystal structure (cf. Fig. 2), may reflect the major significance of dUTPase action in *M. tub.* The Trp fluorescent emission maximum in the His145Trp mutant enzyme is 354 nm (Fig. 3A), a value characteristic for a fully exposed Trp residue available to aqueous solvent. The same was also found in the human Phe158Trp mutant, strengthening the hypothesis that the motif 5 aromatic residue is not secluded in a hydrophobic microenvironment. The fact that Trp replacement of Phe158 in the human enzyme, and His145 in the *M. tub.* dUTPase does not disturb the catalytic activity suggests the importance of an aromatic residue interacting with the uracil ring rather than the exclusiveness of Phe.

We propose that the structurally characterized species-specific segments may be used as docking surfaces for inhibitor candidates with the goal of species-specific inhibition of *M. tub.* dUTPase over the human enzyme.

Since the kinetic properties of the Trp mutant enzyme do not differ from that of the wild-type, this label is also an excellent sensor for following the enzymatic reaction as described in [16] and enables the set-up of large-scale plate assay screening for potential inhibitors. If eventual fluorescent properties of the ligands interfere with this, the optimized sensitive pyrophosphate assay may still be used for large-scale screening and quantitative evaluation of the promising hits.

Acknowledgments

Hungarian Scientific Research Fund (K68229), Howard Hughes Medical Institutes (#55005628 and #55000342), Alexander von Humboldt Foundation, GVOP-3.2.1.-2004-05-0412/3.0 and JÁP-TSZ-071128-TB-INTER from the National Office for Research and Technology, Hungary, FP6 STREP 012127 and FP6 SPINE2c LSHG-CT-2006-031220 from the EU.

Appendix A. Supplementary data

Supplementary data associated with this article can be found, in the online version, at doi:10.1016/j.bbrc.2008.05.130.

References

[1] E.L. Corbett, C.J. Watt, N. Walker, D. Maher, B.G. Williams, M.C. Raviglione, C. Dye, The growing burden of tuberculosis: global trends and interactions with the HIV epidemic, Arch. Intern. Med. 163 (2003) 1009–1021.
[2] K. Blondal, Barriers to reaching the targets for tuberculosis control: multidrug-resistant tuberculosis, Bull. World Health Organ. 85 (2007) 387–390. discussion 391–384.
[3] K.J. Williams, K. Duncan, Current strategies for identifying and validating targets for new treatment-shortening drugs for TB, Curr. Mol. Med. 7 (2007) 297–307.
[4] F.G. Berger, S.H. Berger, Thymidylate synthase as a chemotherapeutic drug target: where are we after fifty years?, Cancer Biol Ther. 5 (2006) 1238–1241.
[5] A.C. Anderson, Targeting DHFR in parasitic protozoa, Drug Discov. Today 10 (2005) 121–128.
[6] R.D. Ladner, The role of dUTPase and uracil-DNA repair in cancer chemotherapy, Curr. Protein Pept. Sci. 2 (2001) 361–370.
[7] J.L. Whittingham, I. Leal, C. Nguyen, G. Kasinathan, E. Bell, A.F. Jones, C. Berry, A. Benito, J.P. Turkenburg, E.J. Dodson, L.M. Ruiz Perez, A.J. Wilkinson, N.G. Johansson, R. Brun, I.H. Gilbert, D. Gonzalez Pacanowska, K.S. Wilson, dUTPase as a platform for antimalarial drug design: structural basis for the selectivity of a class of nucleoside inhibitors, Structure 13 (2005) 329–338.
[8] R. Persson, E.S. Cedergren-Zeppezauer, K.S. Wilson, Homotrimeric dUTPases; structural solutions for specific recognition and hydrolysis of dUTP, Curr. Protein Pept. Sci. 2 (2001) 287–300.
[9] S.S. Helt, M. Thymark, P. Harris, C. Aagaard, J. Dietrich, S. Larsen, M. Willemoes, Mechanism of dTTP inhibition of the bifunctional dCTP deaminase:dUTPase encoded by *Mycobacterium tuberculosis*, J. Mol. Biol. 376 (2008) 554–569.
[10] G. Larsson, L.A. Svensson, P.O. Nyman, Crystal structure of the *Escherichia coli* dUTPase in complex with a substrate analogue (dUDP), Nat. Struct. Biol. 3 (1996) 532–538.
[11] V. Nemeth-Pongracz, O. Barabas, M. Fuxreiter, I. Simon, I. Pichova, M. Rumlova, H. Zabranska, D. Svergun, M. Petoukhov, V. Harmat, E. Klement, E. Hunyadi-Gulyas, K.F. Medzihradszky, E. Konya, B.G. Vertessy, Flexible segments modulate co-folding of dUTPase and nucleocapsid proteins, Nucleic Acids Res. 35 (2007) 495–505.
[12] B. Varga, O. Barabas, J. Kovari, J. Toth, E. Hunyadi-Gulyas, E. Klement, K.F. Medzihradszky, F. Tolgyesi, J. Fidy, B.G. Vertessy, Active site closure facilitates juxtaposition of reactant atoms for initiation of catalysis by human dUTPase, FEBS Lett. 581 (2007) 4783–4788.
[13] S. Chan, B. Segelke, T. Lekin, H. Krupka, U.S. Cho, M.Y. Kim, M. So, C.Y. Kim, C.M. Naranjo, Y.C. Rogers, M.S. Park, G.S. Waldo, I. Pashkov, D. Cascio, J.L. Perry, M.R. Sawaya, Crystal structure of the *Mycobacterium tuberculosis* dUTPase: insights into the catalytic mechanism, J. Mol. Biol. 341 (2004) 503–517.

[14] D.J. McGeoch, Protein sequence comparisons show that the 'pseudoproteases' encoded by poxviruses and certain retroviruses belong to the deoxyuridine triphosphatase family, Nucleic Acids Res. 18 (1990) 4105–4110.
[15] O. Barabas, V. Pongracz, J. Kovari, M. Wilmanns, B.G. Vertessy, Structural insights into the catalytic mechanism of phosphate ester hydrolysis by dUTPase, J. Biol. Chem. 279 (2004) 42907–42915.
[16] J. Toth, B. Varga, M. Kovacs, A. Malnasi-Csizmadia, B.G. Vertessy, Kinetic mechanism of human dUTPase, an essential nucleotide pyrophosphatase enzyme, J. Biol. Chem. 282 (2007) 33572–33582.
[17] M.R. Webb, A continuous spectrophotometric assay for inorganic phosphate and for measuring phosphate release kinetics in biological systems, Proc. Natl. Acad. Sci. USA 89 (1992) 4884–4887.
[18] B. Varga, F. Migliardo, E. Takacs, G.B. Vertessy, S. Magazu, Experimental study on dUTPase-inhibitor candidate and dUTPase/disaccharide mixtures by PCS and ENS, J. Mol. Struct. (in press). Available online 9 November 2007.
[19] A. Vagin, A. Teplyakov, MOLREP: an automated program for molecular replacement, J. Appl. Crystallogr. 30 (1997) 1022–1025.
[20] B.G. Vertessy, P. Zalud, P.O. Nyman, M. Zeppezauer, Identification of tyrosine as a functional residue in the active site of *Escherichia coli* dUTPase, Biochim. Biophys. Acta 1205 (1994) 146–150.
[21] B.G. Vertessy, Flexible glycine rich motif of *Escherichia coli* deoxyuridine triphosphate nucleotidohydrolase is important for functional but not for structural integrity of the enzyme, Proteins 28 (1997) 568–579.
[22] B.G. Vertessy, G. Larsson, T. Persson, A.C. Bergman, R. Persson, P.O. Nyman, The complete triphosphate moiety of non-hydrolyzable substrate analogues is required for a conformational shift of the flexible C-terminus in *E. coli* dUTP pyrophosphatase, FEBS Lett. 421 (1998) 83–88.
[23] C.D. Mol, J.M. Harris, E.M. McIntosh, J.A. Tainer, Human dUTP pyrophosphatase: uracil recognition by a beta hairpin and active sites formed by three separate subunits, Structure 4 (1996) 1077–1092.
[24] G.S. Prasad, E.A. Stura, D.E. McRee, G.S. Laco, C. Hasselkus-Light, J.H. Elder, C.D. Stout, Crystal structure of dUTP pyrophosphatase from feline immunodeficiency virus, Protein Sci. 5 (1996) 2429–2437.
[25] G. Larsson, P.O. Nyman, J.O. Kvassman, Kinetic characterization of dUTPase from *Escherichia coli*, J. Biol. Chem. 271 (1996) 24010–24016.